

WHISTLER MODE STARTUP IN THE MICHIGAN MIRROR MACHINE*

J. Booske^{**}, W. D. Getty, R. M. Gilgenbach, T. Goodman, D. Whaley^{**}, R. Olivieri, E. Pitcher, and L. Simonetti, University of Michigan and R. A. Jong, LLNL

ABSTRACT

Results of investigations of whistler mode ECRH plasma startup in the Michigan Mirror Machine are presented. Electron-velocity-distribution and plasma-spatial-distribution time evolution are characterized by measurements from axially and radially moveable Langmuir probes, an endloss current detector, an electron cyclotron emission radiometer, a foil-filtered X-ray detector, and a diamagnetic loop at the mirror midplane. Measurements of the buildup of both electron density and perpendicular pressure (nkT_{\perp}) are compared to predictions from various numerical models. Both modeling and data suggest the creation of a highly anisotropic electron velocity distribution function with a "sloshing electron" axial density profile.

I. INTRODUCTION

The Michigan Mirror Machine (MIMI) operates as an axisymmetric mirror machine with a 2-to-1 mirror ratio and a midplane field of 2.34 kG. All magnetic field coils are driven with direct current, and the plasma is pulsed at a rate of 40 pulses per minute. This relatively fast repetition rate allows the operator to have almost continuous real-time experimental parameter adjustment for optimizing experimental conditions. Operation thus far has shown good pulse-to-pulse reproducibility.

The apparatus is currently being used to study microwave plasma buildup and plasma heating using the whistler wave mode of propagation. Hydrogen is puffed in near the midplane and ionized as a result of the electron-cyclotron-heating (ECH) microwave pulse. Continuous nitrogen gas flow can also be used. The resonance surfaces are located at $z = 5$ cm. for typical magnetic field strengths. The dynamic gas pressure in the midplane region at the time of the ECH pulse is estimated to be $3-6 \times 10^{-5}$ Torr. This pressure is most important in determining the time scale of the plasma buildup and the maximum stored energy in the plasma.

The plasma buildup process can be divided into three regimes in time. Regime A is a stable startup regime and occurs in the first 200 μ s of the ECH pulse under normal conditions. Regime B is characterized by the appearance of nonthermal microwave emission which has been tentatively identified with the velocity-anisotropy-driven whistler instability. Regime C is dominated by an MHD instability, plasma axial expansion, and plasma cooling. The present paper is primarily concerned with Regime A. Details about all three regimes are given in Reference 1.

II. DESCRIPTION OF APPARATUS

A schematic drawing of the apparatus is shown in Figure 1. The basic vacuum system consists of a 10-cm diameter, 126-cm long plasma chamber with a 46-cm diameter tank at one end. The axial distance between mirror peaks is 49 cm. The ECH pulse is launched from a dielectric-loaded horn antenna located in the endtank. The heating frequency is 7.43 GHz, the peak power is 1000 W, and the pulse length is 400 μ s. The dynamic gas distribution is such that very little gas is present at the outermost resonance surface and no plasma is produced there, making the inner resonance accessible from the high-field side. This arrangement makes the whistler mode very effective for resonance heating.

A second dielectric-loaded horn antenna is located at the opposite end of the vacuum tube and is used to detect plasma emission and transmitted microwave heating power. The dielectric-loaded antennas have a narrower radiation pattern than a standard horn, thereby improving their selectivity for transmitting and receiving the whistler mode. In addition to plasma emission and ECH transmitted power, ECH incident and reflected power on the transmitting side are also measured.

Plasma diagnostics consist of a midplane diamagnetic loop, an 8-mm transmission interferometer, an electron-cyclotron-emission radiometer for detecting whistler-wave cyclotron emission (WECE), a foil-filtered X-ray detector, an axially and azimuthally moveable Langmuir probe, and an endloss current collector. The WECE radiometer is protected from the heating pulse by a notch filter. The endloss detector consists of a single grounded entrance grid and a biased collector. It receives current from a flux tube that intersects the midplane at a radius of approximately 2.5 cm. The X-ray detector has thus far been used with 7 μ m and 25 μ m foils.

III. EXPERIMENTAL RESULTS

In the stable buildup regime, experimental and theoretical results indicate that the plasma forms a "sloshing electron" velocity distribution with a midplane pitch angle of approximately 70 degrees. The diamagnetic signal rises rapidly to a peak in the range of 10^{14} eV/cm³ and the plasma potential is negative with off-midplane negative peaks, indicating good heating and confinement of electrons. Incident ECH power does not change, but transmitted power falls significantly to a negligible level as the plasma stored energy increases. The rate of increase of the stored energy is consistent with the absorption of all of the incident ECH power. Microwave absorbing liners have been inserted in various positions inside the vacuum system to ascertain that cavity modes are unimportant, thus verifying total single-pass absorption.

The stable buildup regime is terminated by a burst of WECE at a frequency below the midplane cyclotron frequency. The WECE burst is 10 to 20 dB above the background level of doppler-shifted emission by the sloshing electrons. Thermal emission at frequencies above the midplane cyclotron frequency is also observed during Regime A, and is due to relatively cold electrons trapped near the midplane by the negative-potential peaks produced off the midplane by the sloshing electrons.

The microwave interferometer is located at a cross-section 11 cm from the midplane, which is outboard of the resonance surface, and does not detect plasma until instabilities occur at the end of Regime A and the plasma expands axially. Similarly, no endloss current is detected.

The floating potential near the midplane when the whistler instability occurs (Regime B) and later in Regime C is shown in Figure 2. The probe's radial position is changed by rotating it clockwise (CW) or counterclockwise (CCW). Slightly different curves are obtained because the ECH antenna is not concentric with the vacuum vessel. The plasma potential is negative in Regimes A and B, as shown in the lower curves in Figure 2, but within approximately 25 μ s turns positive in Regime C as shown by the upper curves. Since the potential must go to zero at the vessel wall ($r = 5$ cm), the probe results indicate that the peak negative potential occurs off axis at a radius of 4.5 cm, whereas the positive potential peaks on the axis. The off-axis negative peak indicates a predominance of electrons off axis as the plasma leaves Regime A and enters Regime B.

Typical X-ray signals are shown in Figure 3 for three different neutral gas pressures in the midplane region. At high pressure the hot-electron component of the plasma is smaller and the X-ray and diamagnetic signals are small. At lower pressures the peaks of the X-ray and diamagnetism signals appear later and are much larger. The low pressure cases shown in Figure 3 can exhibit earlier peaks under different conditions that are believed to be related to scrape-off of hot electrons on the probe and to the position of the resonance surface. These conditions are currently being studied. Preliminary results from foil absorption measurements indicate hot-electron energies of 1 to 2 keV.

Evidence for the existence of the sloshing electron velocity distribution is obtained from the axial density profile and the WECE spectrum. Fokker-Planck calculations have been done to verify the existence of this distribution for parameters similar to those of the experiment. Based on the Fokker-Planck results, a model sloshing-electron velocity distribution function was developed¹ for use in a WECE computer code developed by Tsakiris and Ellis². A cold plasma component was added to the sloshing-electron component. Both were found to be necessary to produce satisfactory agreement between the measured and calculated spectra. The self-consistent axial density profile used for the WECE calculation is shown in Figure 4 along with the measured density profile. The measured profile is in qualitative agreement with the predicted off-midplane density peaks.

IV. COMPUTER BUILDUP CALCULATIONS

Computer simulations of the ECRH startup have been performed using the Michigan ECRH Startup and Heating Rate Equation Code (MESHREC). MESHREC is based on rate equations for density and energy of electron energy groups. The fundamental modeling physics are derived from the transport of electrons in velocity space. Derivations of the rate equations begin with a bounce-averaged kinetic equation of the form:

$$\frac{\partial f}{\partial t} = -\frac{\partial}{\partial v} \cdot \left[G f + D \frac{\partial f}{\partial v} \right] \quad (1)$$

where G and D represent velocity space drag and diffusion coefficients, respectively.

Electron transport is assumed to result from collisions (with other electrons, neutrals, and

ions) and rf diffusion. Collisional velocity space transport coefficients were derived from standard Rutherford scattering theory. RF diffusion coefficients were derived from the impulse heating model of Jaeger, et. al.³ Two energy groups (colds, hot) of electrons were assumed, with cold electrons resulting from impact ionization of neutrals. Explicit expressions for Eq. (1) require specification of electron velocity distribution functions. For this the cold electrons were assumed to have a Maxwellian distribution with empty loss cone and the hot electrons were given a sloshing electron distribution¹. With this information, rate equations for electron density and energy were obtained from the zeroth and second-order velocity moments of Eq. (1). Ion density was computed as a function of time by assuming quasineutrality, $n_i = n_c + n_h$. Electrostatic potentials were neglected for the results presented here.

Initial conditions were chosen as $n_c(0) = n_h(0) = 10^9 \text{ cm}^{-3}$, $T_c(0) = 20 \text{ eV}$, and $T_h(0) = 200 \text{ eV}$. These conditions are representative of values expected at the beginning of diamagnetism buildup. In Figure 5 sample MESHREC results are presented for total density and diamagnetism. For these runs the working gas was assumed to be nitrogen with initial pressures of 0.1 and 0.01 mTorr. The results of the calculation show several features relevant to the experiment. First, the rate of diamagnetism buildup depends sensitively on the neutral pressure. This agrees with experimental findings and is a consequence of the fact that at lower neutral densities (corresponding to lower ionization rates), the hot-electron energy increases rapidly. This causes an even greater decrease of the energy dependent ionization rate, resulting in slower buildup of electron density as shown in Figure 5.

A second result of the simulation concerns the prediction that typical experimental startup characteristics are obtained with lower neutral pressures than those used experimentally. In particular, the startup results presented in Figure 5 at 0.1 mTorr were experimentally achieved with nitrogen gas pressures of approximately 0.02 mTorr. It is not yet clear why this disagreement between theory and experiment exists.

The preliminary results from MESHREC are in rough agreement with results from sophisticated Fokker-Planck simulations being done at Lawrence Livermore National Laboratory.

REFERENCES

1. J. H. Booske, W. D. Getty, R. M. Gilgenbach, and R. A. Jong, Phys. Fluids (to be published).
2. G. D. Tsakiris and R. F. Ellis, Nucl. Fusion 23, 1115 (1983).
3. F. Jaeger, A. J. Lichtenberg, and M. A. Lieberman, Plasma Phys. 14, 1073 (1972).

*Work supported by NSF.

*Supported by DOE MFE Technology Fellowship.

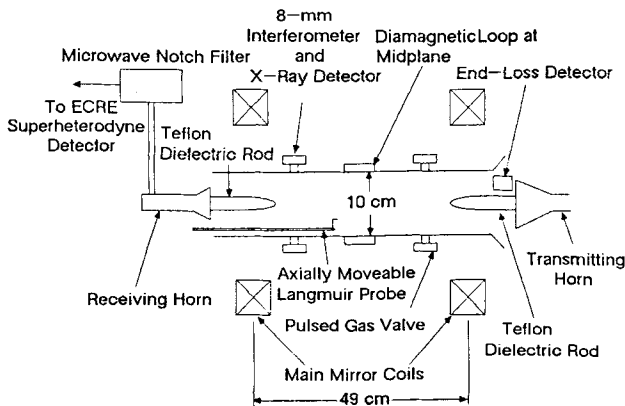


Fig. 1 Main features of the Michigan Mirror Machine (MIMI).

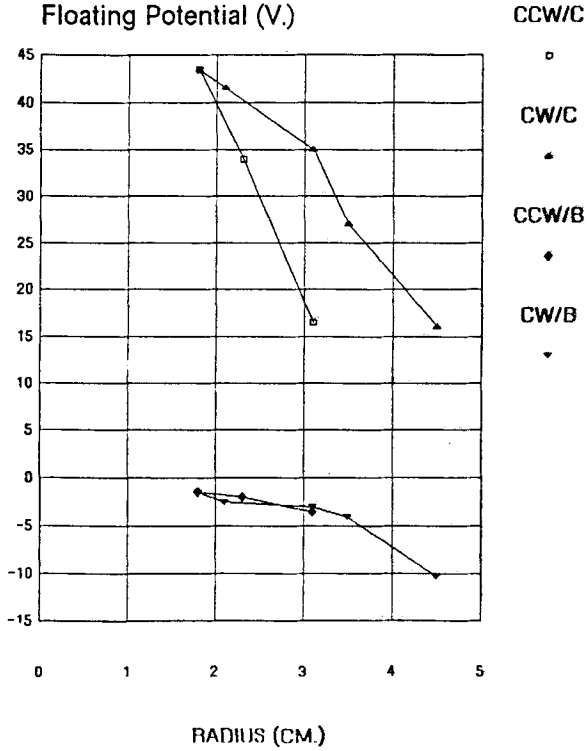


Fig. 2 Floating potential radial profiles near the midplane for Regime B (CCW/B and CW/B) and Regime C (CCW/C and CW/C). CCW and CW refer to the directions of azimuthal rotation of the probe; rotation changes the probe's radial position. The vessel wall is at $r = 5$ cm.

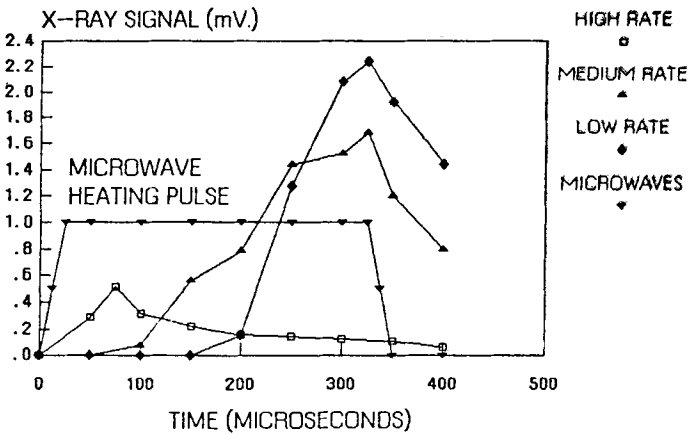


Fig. 3 X-ray signals for high, medium, and low neutral gas source rates (i.e., pressure at the time of the ECH pulse). The incident ECH microwave pulse is also shown.

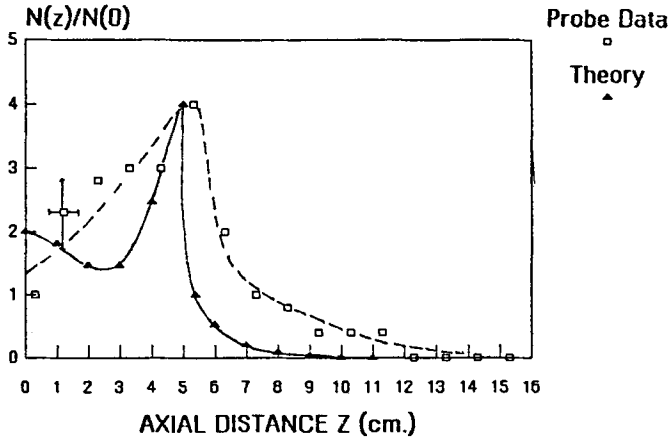


Fig. 4 Axial dependence of relative electron density as measured by a Langmuir probe biased in the electron saturation regime at +100 V. The plasma buildup is in Regime A at $t = 145 \mu\text{s}$ for these data. The theoretical curve is for the sloshing electron density plus the cold electron density axial distributions needed to match the observed WECE spectrum.

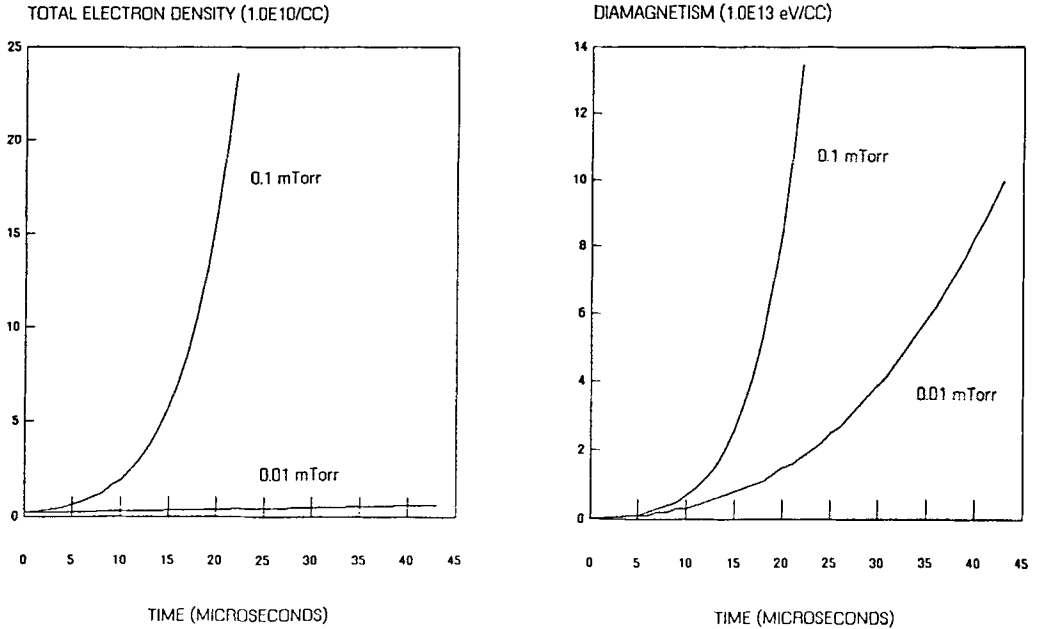


Fig. 5 Computer simulation results from MESHREC for diamagnetism and total electron density buildup at two different gas pressures.